

1
2
3
4
5
6
7
8
9
10
11
12
13
14
15
16
17
18
19
20
21
22
23
24
25
26
27
28
29

Optimizing the cementitious immobilization of boron isotopes in simulated borate radioactive liquid waste with different ratios of cement blends

Gabriel I. Iklaga^{1*}, Mojtaba Rostamiparsa¹, István Tolnai², Nándor Kaposy²,
Katalin Gméling², Emese Csipa²,
Csaba Tóbi², Viktória Gável³, Péter Kónya⁴, Csaba Szabó¹, Margit Fábián², Zsuzsanna
Szabó-Krausz¹, Péter Völgyesi²

¹*Lithosphere Fluid Research Laboratory, Institute of Geography and Earth Sciences Eötvös Loránd University, Budapest, Hungary*

²*HUN-REN Centre for Energy Research, Konkoly-Thege Miklós út. 29-33, 1121, Budapest, Hungary*

³*CEMKUT Cementipari Research Development Limited, Bécsi út 122-124, 1034 Budapest, Hungary*

⁴*Geological Institute of Hungary, Stefania ut. 14, 1143, Budapest, Hungary*

30 **Abstract**

31 Nuclear power plants use boric acid (a high-volume liquid waste) with different ^{10}B enrichment
32 levels (from natural ratio to 90% ^{10}B) as neutron absorber. In this study, we aimed to find the
33 optimal ratio of ordinary Portland cement and sulfoaluminate cement blend to improve the
34 mechanical and chemical durability of final waste forms for borate immobilization. The results
35 indicated that the blend ratio of 20% sulfoaluminate cement to 80% ordinary Portland cement
36 showed the best physical stability and lowest boron isotopic leachability from the final waste
37 form.

38 **Keywords:** Cementitious immobilization; Boron isotopes; Ordinary Portland cement;
39 Sulfoaluminate cement

40

41 **1. Introduction**

42 Global energy demand has been on exponentially continuous increase in recent times, which
43 has sparked governments' and researchers' interest in terms of accessing efficient and
44 sustainable energy systems [1]. The demand for energy resources to conduct socioeconomic
45 activities by the increasing global human population has also led to significant increase of
46 environmental pollution associated with the use of fossil fuels [2], [3]. The challenge of
47 pollution from fossil fuel usage has necessitated the need to shift to cleaner energy alternatives
48 such as nuclear energy. However, radioactive waste is produced during the proliferation of
49 nuclear energy from nuclear power plants (NPP) [4]. Boric acid waste is considered to be the
50 highest volume liquid waste residue streaming from NPPs [5]–[8]. The potent capacity of ^{10}B
51 isotope for neutron adsorption in nuclear reactor systems has led to the widespread usage of
52 boric acid solutions in nuclear technology. However, some technical limitations of boric acid,
53 like the corrosive impact within NPP operation loops and significant leachability of boron from
54 their final cementitious waste forms, have prompted researchers to develop better neutron
55 absorbers [9]. In this context, some NPP in France, Germany, Japan, the United States, China
56 and India have started to use enriched boric acid (EBA) which allows to reduce the volume of
57 this solution therefore to limit its negative impacts.

58 Natural boric acid (NBA) has a ^{10}B abundance of about 20%, and ^{11}B abundance of 80%.
59 Enriched boric acid (EBA) in use may be enriched up to 90% ^{10}B to utilize the notable cross-
60 sectional difference between the two stable boron isotopes ($\sigma_{B-10}=3837$ barn and $\sigma_{B-11}=0.005$
61 barn). Our previous study had revealed by Raman-spectrometry that simulated borate liquid

62 wastes of NBA and EBA contain different molecular forms of boron [10]. Therefore, the
63 different interactions with ordinary Portland cements (OPC) clinkers consequently cause
64 different mineralogy and therefore stability and durability of final waste forms [13]. On the
65 other hand, sulfoaluminate cement (SAC) has shown promising results as a new cementitious
66 matrix to enhance mechanical stability and lower boron leachability to immobilize the boric
67 acid wastes solutions [11], [12]. However, due to SAC's unstable characteristics when used
68 unblended with another cement type, it has been applied as an additive to the OPC matrices to
69 enhance initial strength and setting properties [13], [14].

70 This study has assessed the effects of blending different ratios of SAC in OPC for optimizing
71 the chemical and mechanical stability for immobilizing of both NBA and EBA. At first, 0 -40%
72 SAC was added to OPC to prepare the simulated waste forms [10]. Then both the elemental
73 and isotopic leachability of boron from the solidified final waste forms were measured in a
74 standardized leaching test introduced in ASTM C1308-21 [15] by inductively coupled plasma
75 optical emission spectroscopy (ICP-OES) and inductively coupled plasma mass spectroscopy
76 (ICP-MS). The mechanical and chemical properties of the cementitious solid matrices before
77 and after the leaching tests were studied with scanning electron microscopy (SEM), X-ray
78 diffraction (XRD), prompt-gamma neutron activation analysis (PGAA).

79

80 **2. Experiments**

81 The experimental strategy used in this study include: 1) preparation of the simulated NBA- and
82 EBA-liquid radioactive wastes; 2) preparation of simulated solidified cement waste forms; 3)
83 running the standardized leaching tests; 4) performing the mechanical, mineralogical,
84 morphological, elemental analyses on the solidified cement pastes before and after the leaching;
85 and 5) elemental and isotopic analyses of the leachates derived from the leaching test.

86

87 **2.1. Preparation and characterization the simulated NBA and EBA liquid** 88 **wastes**

89 To simulate the high-volume boric acid liquid waste in NPP evaporated sludge, 40 g of natural
90 boric acid (NBA with 20% ^{10}B , CAS: 1333-73-9 NUKEM) and 40 g of enriched boric acid
91 (EBA with $^{10}\text{B}>95\%$, CAS: 13813-79-1, Aldirich) powders were mixed with 1-liter
92 demineralized (DM) water (conductivity=1.1 S/cm, pH=7.5 at 23 °C) [13]. To make boric acid
93 more soluble in DM water and to lessen the acid's ability to delay the setting of cement, granular
94 sodium hydroxide (NaOH with 99.2% purity, CAS: 1310-73-2, AnalaR NORMAPUR, VWR

95 Bdh chemical product) was utilized to neutralize the simulated waste solutions in a 1.25
 96 $H_3BO_3/NaOH$ molar ratio [13]. The reaction between the acid and base produces an alkaline
 97 pH solution, which optimizes the setting and hardening of cement paste [16]. Specifications of
 98 the simulated liquid boric acid waste solutions used for the study are summarized in Table 1.

Sample name	Mixing solvent	Mixing solute	Boron concentration (g/l)	^{10}B enrichment
MR: reference solution made with DM water of 2 ppb purity	DM water	-	0	-
ME: waste solution made from mixture of DM water and enriched boric acid solute	DM water	EBA: enriched boric acid	40	95 % (enriched)
MN: waste solution made from mixture of DM water and natural boric acid solute	DM water	NBA: natural boric acid solute	40	19.8 % (natural)

99 **Table 1:** Specifications of simulated liquid boric acid waste solutions.
 100

101 2.2. Preparation the simulated solid waste forms

102 2.2.1. Chemical compositions of cements

103 The simulated solidified cement pastes samples (waste forms) were made using OPC (grade R
 104 – 15796 CEM I 52.5 N) and SAC (grade R – 14734 ALI CEM GREEN) from CEMKUT Ltd,
 105 with given chemical compositions of major elements and mineral phase compositions specified
 106 in Table 2.

Chemical compositions of major elements in OPC and SAC clinkers												
Oxides	SiO ₂	Al ₂ O ₃	Fe ₂ O ₃	CaO	MgO	K ₂ O	Na ₂ O	SO ₃	Cl ⁻	TiO ₂	IR	LOI
weight percentage (m/m %) in OPC	19.21	5.83	3.62	65.75	2.40	0.26	0.02	3.43	0.02	0	0	1.26
weight percentage (m/m %) in SAC	6.18	23.49	1.28	36.64	4.80	0.36	0.75	21.54	0	0.36	0.94	0.70
Solid phase composition												
Mineralogical name (technical formula)	alite (C ₃ S)	belite (C ₂ S)	aluminat (C ₃ A)	ye'elimit (C ₄ A ₃ S̄)	ferrite (C ₄ AF)	anhydrite (C \bar{S})						
chemical formula	Ca ₃ SiO ₅	Ca ₂ SiO ₄	Ca ₃ Al ₂ O ₆	Ca ₄ (AlO ₂) ₆ SO ₄	Ca ₄ Al ₂ Fe ₂ O ₁₀	CaSO ₄						
weight percentage (m/m %) in OPC	57.5	11.8	9.3	0	11.0	5.8						
weight percentage (m/m %) in SAC	1.7	44.6	0	16.1	13.2	24.4						

107 **Table 2:** Chemical and mineralogy specifications of ordinary Portland cement (OPC) and
 108 sulfoaluminate cement (SAC) pastes provided by CEMKUT Ltd. (LOI: loss on ignition; IR:
 109 insoluble residue)

110

111 2.2.2. Preparation of cement paste samples

112 The required ratios of OPC and SAC cement clinker (SAC contribution with 0, 10, 20, 30 and
 113 40%) shown in supplementary tables 1a & 1b were weighed and put into a mixer (HAUSER
 114 DM-601) before the NBA or EBA simulated liquid boric acid wastes or DM water was added
 115 to the cement powder at a 0.4 water-to-cement ratio (W/C) to mix cement pastes. To create a
 116 homogeneous paste, the mixture was mechanically whisked (90 rotations-per-minute for 12
 117 min) under conditions available in the laboratory ($T = 23\text{ }^{\circ}\text{C}$, Relative humidity = 70%).

118 The cement pastes were then loaded into light density polyethylene (LDPE) cylindrical tubes
 119 of 43×25 mm dimensions. To remove air bubbles, the molds were shaken for 5 minutes
 120 manually [13]. The molds were then placed in a temperature-controlled incubator (VWR-
 121 INCU Line 68R) adjusted to a constant 20°C . After curing the samples for 28 days, the
 122 cylindrical plastic tubes were lightly pilled off the cement paste without scratching the sample
 123 surface using a sharp office blade/cutter.

Series Code	OPC content (%)	SAC content (%)	Enrichment of solution
MR0	100	0	DM water
MR1	90	10	DM water
MR2	80	20	DM water
MR3	70	30	DM water
MR4	60	40	DM water
MN0	100	0	NBA (^{11}B)
MN1	90	10	NBA (^{11}B)
MN2	80	20	NBA (^{11}B)
MN3	70	30	NBA (^{11}B)
MN4	60	40	NBA (^{11}B)
ME0	100	0	EBA (^{10}B)
ME1	90	10	EBA (^{10}B)
ME2	80	20	EBA (^{10}B)
ME3	70	30	EBA (^{10}B)
ME4	60	40	EBA (^{10}B)

124 **Supplementary table 1a:** Naming convention for Solid Cement Samples before leaching
 125 test. Where: MR series are reference samples before leaching, MN series are ^{11}B immobilized
 126 cement paste samples before leaching and ME series are ^{10}B immobilized cement paste
 127 samples before leaching.

128

129

130

Series Code	OPC content (%)	SAC content (%)	Enrichment of solution
LMR0	100	0	DM water
LMR1	90	10	DM water

LMR2	80	20	DM water
LMR3	70	30	DM water
LMR4	60	40	DM water
LMN0	100	0	NBA (¹¹ B)
LMN1	90	10	NBA (¹¹ B)
LMN2	80	20	NBA (¹¹ B)
LMN3	70	30	NBA (¹¹ B)
LMN4	60	40	NBA (¹¹ B)
LME0	100	0	EBA (¹⁰ B)
LME1	90	10	EBA (¹⁰ B)
LME2	80	20	EBA (¹⁰ B)
LME3	70	30	EBA (¹⁰ B)
LME4	60	40	EBA (¹⁰ B)

131 **Supplementary table 1b:** Naming convention for Solid Cement Samples after leaching test.
 132 Where: LMR series are reference samples after leaching, LMN series are ¹¹B immobilized
 133 cement paste samples after leaching and LME series are ¹⁰B immobilized cement paste samples
 134 after leaching.

135

136 **2.3. Leaching tests**

137 Standardized leaching test experiments were conducted in accordance with the guidelines in
 138 American society for testing and materials ASTM C1308-21 [15]. The cylindrical solid samples
 139 with a 50 cm² contact surface were submerged in 500 ml DM water (leachant), and the resulting
 140 solutions (leachates) were changed and sampled at 2, 5, 17, and 24 hours and then daily for the
 141 next 10 days [10].

142 **2.4. Analyses of the leachates**

143 After running the leaching test, all leachates were acidified with ultrapure nitric acid (70%,
 144 purified by redistillation, $\geq 99.999\%$ trace metal basis; CAS Number: 7697-37-2 Sigma-
 145 Aldrich) and then filtered through a cellulose acetate membrane with a 0.45 μm pore size
 146 (FILTER BIO; pore diameter of 0.45 μm). All samples then were analyzed to determine the
 147 elemental boron concentration and its ¹⁰B/¹¹B isotopic ratio by using ICP-OES; Perkin Elmer
 148 Avio 200 and ICP-MS; Thermo Finnigan-Element2.

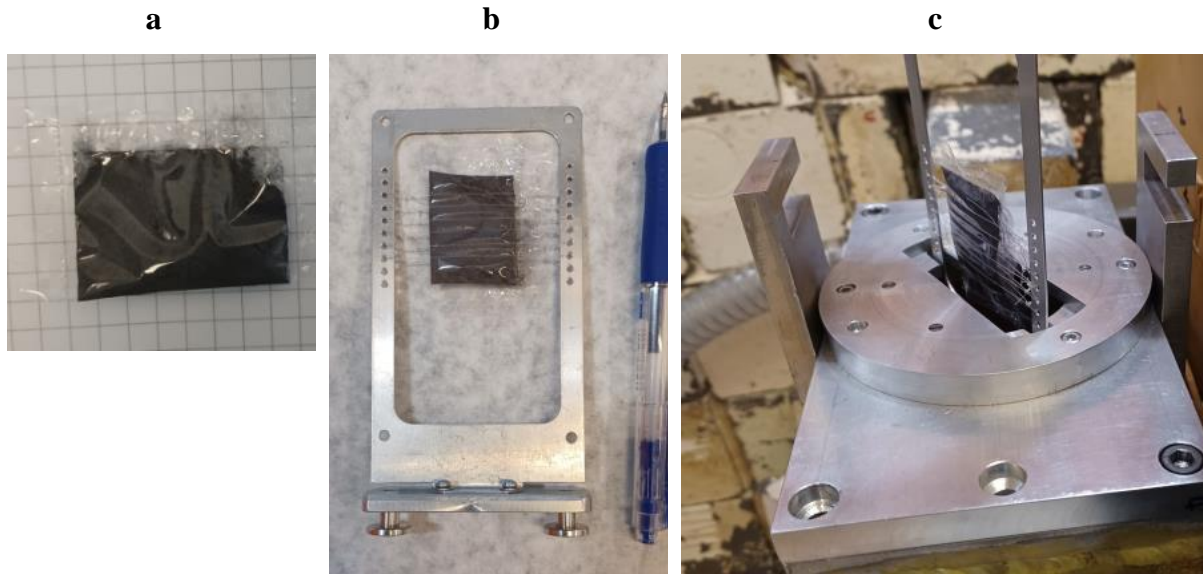
149 **2.5. Chemical and phase composition of the cementitious specimens**

150 Before and after the leaching tests, all types of cylindrical solidified wastefoms were subjected
 151 to morphological, elemental, and mineralogical analyses. This was for evaluating the impact of
 152 applying the simulated liquid wastes with different boron enrichments and different
 153 concentrations of SAC on the results of the leaching phenomenon on the solidified specimens.
 154 The cylindrical cement samples were split in half, their internal rims were polished using

155 Buehler silicon carbide paper (grit 500), and then analyzed using scanning electron microscopy
156 (SEM). The outer rims (surface area which was in direct contact with the leachate) of all the
157 leached and untreated solidified specimens were scraped-off, powdered to achieve the grain
158 size below $\sim 63 \mu\text{m}$ and measured with X-ray diffraction (XRD).

159 After the SEM measurements using the threshold brightness histogram technique approach, the
160 ImageJ image processing software (version 1.38e/Java 1.5.0_09) was utilized to quantify the
161 total surface area of the SEM-BSE pictures of the cement paste samples covered by unreacted
162 clinker [17]. Each of the samples were measured three times to obtain the uncertainty values,
163 with an average uncertainty percentage of 8%. QGIS software was used to measure the macro-
164 fractures on the SEM-BSE images of the NBA, EBA, and reference cement-paste samples.
165 Following the conversion of the image pixel scale to the designated SEM-BSE image scale, the
166 surface macro-fractures and total lengths of the line (fractures) networks on the samples were
167 measured using the line vectorization and quantification algorithm tools.

168 PGAA is a great non-destructive method to measure boron content of bulk samples without
169 sample preparation, and the results are not influenced by the matrix effect. As ^{10}B has a high
170 neutron capture cross section and significant prompt-gamma emission, that it is easy to
171 recognize in the prompt-gamma spectra, however the doppler broadened peak causing a little
172 modified peak-fitting method and peak are calculation with corresponding corrections [18].
173 The OPC and SAC cement blend powder before and after the leaching tests were also
174 characterized using the prompt – gamma activation analysis (PGAA) technique. For this
175 analysis about 4g portions were weighed and sealed into a Teflon bag. The samples were
176 examined at temperature 20°C with prepared sample bags roughly $20 \times 30 \times 3 \text{ mm}$ in size as
177 shown in Figure S2. At the PGAA station's sample site, the neutron flux was approximately
178 $9.6 \times 10^7 \text{ cm}^{-2}\text{s}^{-1}$. The neutron beam's cross-section was $20 \times 20 \text{ mm}^2$. A High-Purity Germanium
179 (HPGe) detector with a Bismuth Germanate (BGO) scintillator and 10 cm thick lead shielding
180 was used to measure the energy and intensity of the characteristic gamma ray emitted by each
181 element in the samples during the neutron capture process. An Ortec, model DSPEC 502A
182 digital spectrometer, was used to process the signals. The element identification and
183 quantification were done with the ProSpeRo program [19], utilizing an in-house developed and
184 validated prompt-gamma analysis library [18]. The background of the beam has been
185 sufficiently corrected [19].



186 **Fig. S2:** the samples were sealed into a Teflon (FEP) bag (a) and fixed in an aluminium sample
 187 holder frame with Teflon strings (b). The samples are placed into the PGAA sample chamber
 188 into the cold neutron beam for irradiation.

189

190 2.6. Other calculation methods

191 *Incremental fraction leached (IFL):* The unitless incremental fraction leached (IFL_n) of boron
 192 during the n^{th} test interval is computed following the standardized approach as shown in
 193 equation 1:

$$194 \quad IFL_n = \alpha_n^B / A_0^B \quad (1)$$

195 where α_n^B (mg/l) is the amount of boron determined in the n^{th} test interval's leachate, A_0^B (mg/l)
 196 is the amount of boron present in the consolidated material before the test (Table S1).

197 *Cumulative fraction leached (CFL):* The cumulative fraction of boron that has been leached
 198 (CFL_j) up until the j^{th} interval is determined by equation 2:

$$199 \quad CFL_j = \sum_{n=1}^j \alpha_n^B / A_0^B = \sum_{n=1}^j IFL_n \quad (2)$$

200 Standardized leaching test data from the various solidified cementitious samples can be easily
 201 compared graphically by plotting the CFL values with the cumulative time. These findings can
 202 be utilized later to forecast the long-term leaching behavior, as well as the general robustness
 203 and performance of the ultimate waste forms [15].

204

205 2.7. Mechanical strength tests of the solid cementitious specimens

206 The cement pastes both before and after the standardized leaching test were investigated by

207 mechanical test (standardized compressive strength test).

208 Before the test, the specimens were stored in a climate-controlled room followed by the
209 standard of the European Standard EN 196-1:2016 (temperature: $20,0 \pm 1,0^\circ\text{C}$, relative humidity:
210 $\geq 90\%$) [20]. The compressive strength was tested using a calibrated pressing machine
211 (producer: Toni Technik Baustoffprüfsysteme GmbH). A calibrated digital caliper was utilized
212 as the geometry measuring equipment and a calibrated digital laboratory scale was used as the
213 mass measuring tool for the samples. Every gadget in use complied with European Standard
214 EN 196-1:2016.

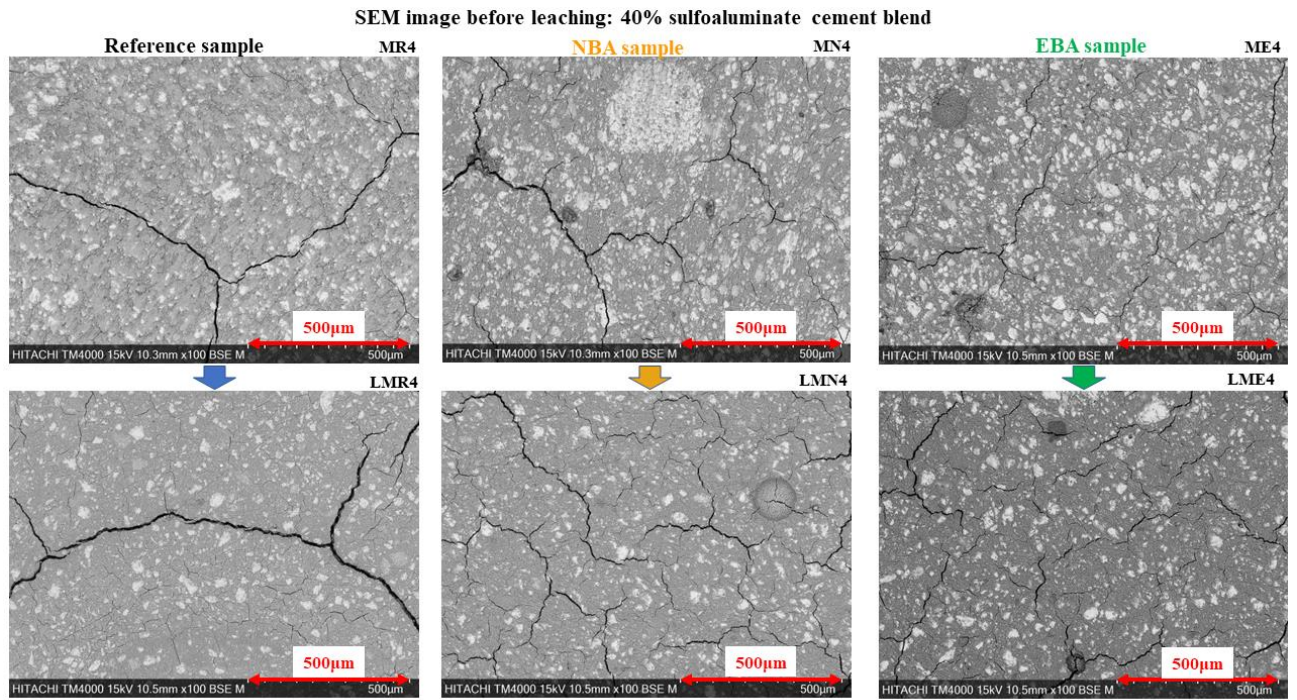
215

216 **3. Results**

217 **3.1. Results of SEM measurements on the cementitious samples**

218 Results of the semiquantitative SEM-BSE measurements of the solidified cement paste samples
219 was used to assess the morphological variations between the reference, NBA and EBA samples
220 before and after the standardized leaching test (Fig. 1). By measuring the cross-sectional area
221 of the unreacted bright (white) clinker minerals and macro-fracture lengths on the surface of
222 the cement paste samples, the cement mixture with the least surface fractures and surface area
223 was identified as the samples with the maximum percentage of the SAC addition (40%).

224 The unreacted bright (white) clinker minerals observed on the solidified samples surface in the
225 SEM-BSE images (bright phases) were used as an index for assessing the effect of SAC
226 addition and boric acid wastewater (NBA and EBA) on the hydration rates of each sample
227 blend.



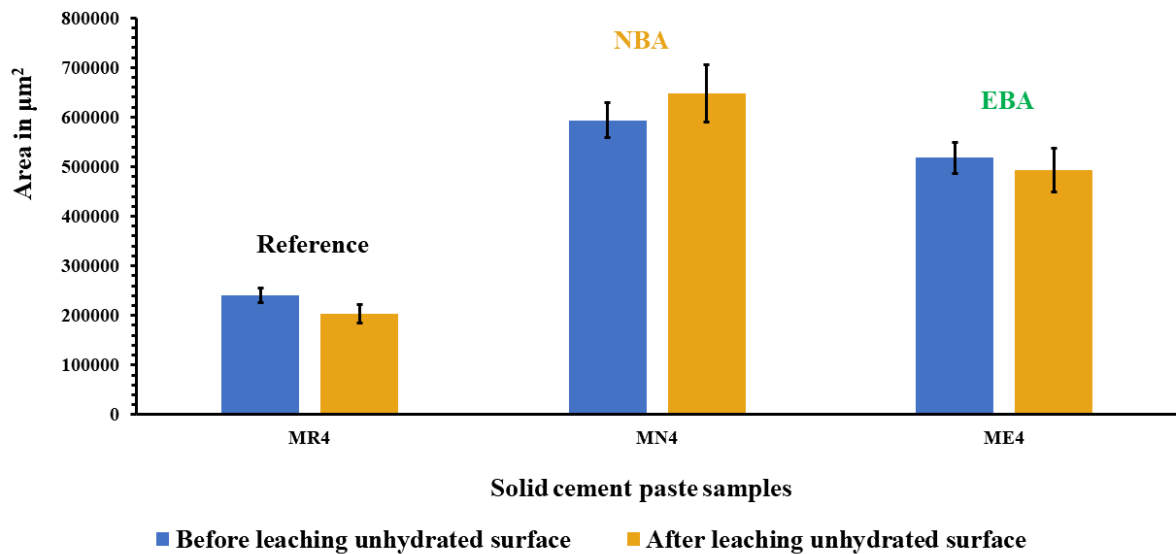
228
229
230
231
232
233
234

SEM image after leaching: 40% sulfoaluminate cement blend

Fig. 1 SEM-BSE images showing surface morphologies of reference, NBA and EBA cement paste samples containing 40% SAC blend before and after the standardized leaching test. MR = cement paste mixed with DM water; MN = cement paste mixed with natural boric acid; ME = cement paste mixed with enriched boric acid; L = cement paste after standardized leaching test; and 4 = 40% SAC in the cement paste.

235 The result of the selected blend, with 40% SAC addition, showed that the NBA cement-paste
236 wastefoms (MN4) showed the biggest total surface cross-sectional area of unreacted clinker
237 minerals while the reference (MR4) cement-paste samples showed the least unreacted clinker
238 minerals surface cover as summarized in Fig. 2.

SEM result summary indicating unhydrated surface area of solid cement samples before and after leaching

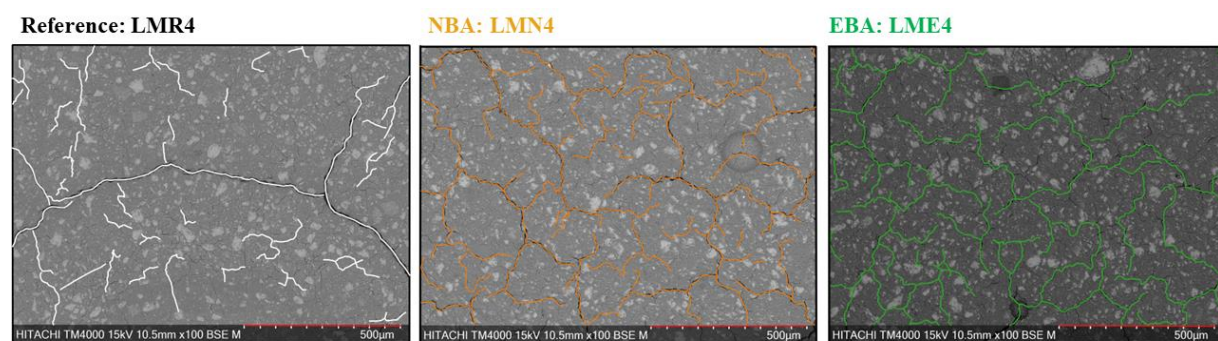


239
240
241
242
243
244

Fig. 2 Surface area measurement analyses indicating unreacted clinker minerals (white bright phases in Fig. 1) using ImageJ software. The measurement has an average percentage uncertainty of 8% from three measurements taken per sample.

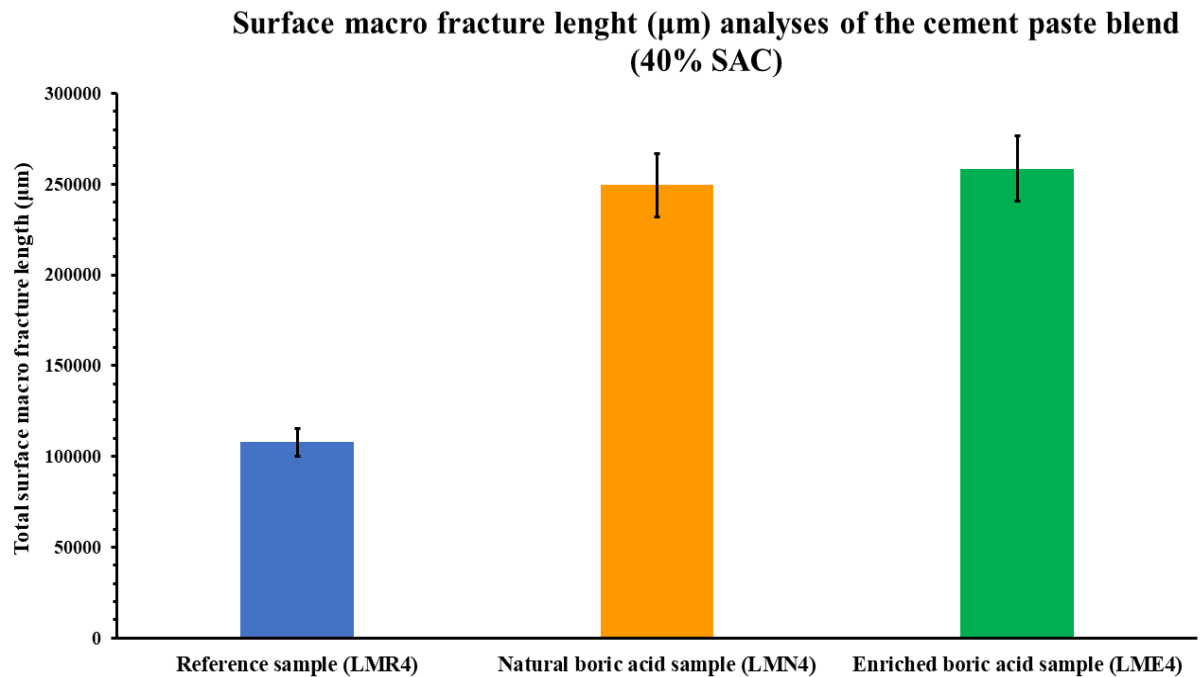
245
246
247
248
249

The results showed that the total length of macro-fractures on the reference cement paste sample LMR4 was $107\,856 \pm 7\,550 \mu\text{m}$. The total surface macro-fracture length on the NBA cement paste sample LMN4 was $249\,305 \pm 17\,451 \mu\text{m}$, while the total surface macro-fracture length on the EBA cement paste sample LME4 was $258\,432 \pm 18\,090 \mu\text{m}$ as shown in Figs. 3 and 4.



250
251
252
253

Fig. 3 SEM-BSE images surface macro fracture length measurement analyses of the reference, NBA and EBA cement paste samples (40% SAC blend) after the standardized leaching test using QGIS software.



254
255

256 **Fig. 4** SEM-BSE images surface macro fracture length measurement analyses graph of the
257 reference, NBA and EBA cement paste samples (40% SAC) after the standardized leaching test
258 using QGIS software. The measurement has an average relative uncertainty of 7 % from three
259 measurements taken per sample.

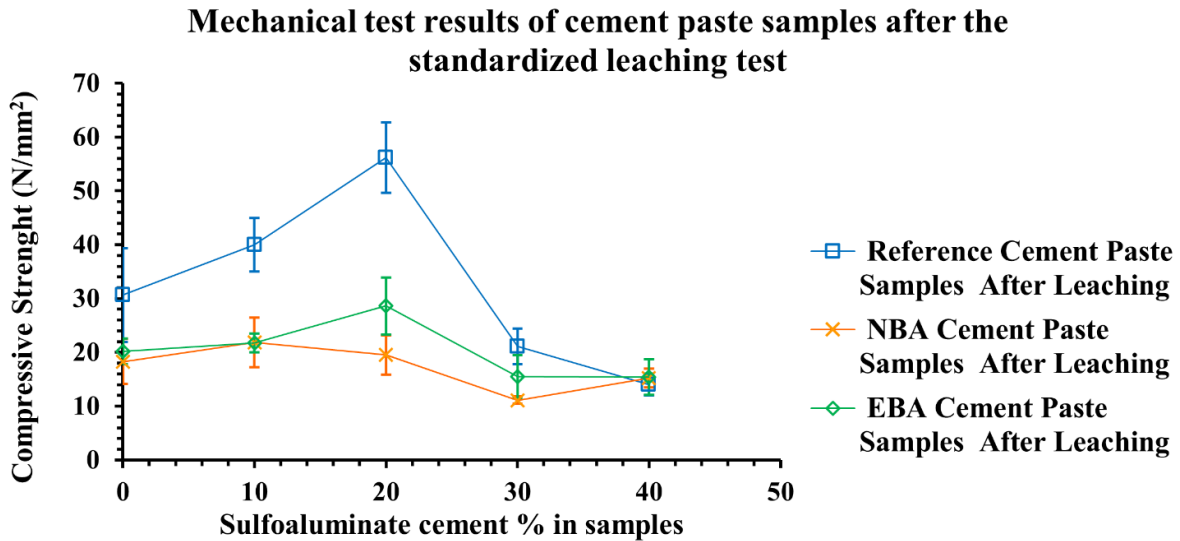
260

261

262 **3.2. Results of the mechanical test of the cement paste samples**

263 The compressive strength test on the cement paste samples (Fig. 5) indicated that up to 30 %
264 SAC content in the blend, the reference cement paste samples showed higher compressive
265 strength value than both the NBA and EBA cement paste samples. The highest compressive
266 strength value for the reference cement paste have been measured to be approximately 56
267 N/mm^2 with 20 % SAC addition, after the standardized leaching test.

268 A comparison between the NBA and EBA samples indicated that the EBA cement paste
269 samples had the highest compressive strength value of approx. 38 N/mm^2 with 20% SAC
270 addition, while the NBA cement paste samples' highest compressive strength value was lower,
271 only 20 N/mm^2 with 10% SAC ratio in the blend. Furthermore, the results showed a significant
272 compressive strength value decrease with the increase of SAC percentage beyond the 20 %
273 SAC blend mark. The uncertainties were obtained from the compressive strength values of the
274 4 replicates of each cement mixture type.



275

276

277

278

279 **Fig. 5** Mechanical (compressive strength) test results for the cement paste samples after the
 280 standardized leaching test, indicating 0, 10, 20, 30 and 40 % SAC-blend in cement mixed with
 281 DM water, NBA and EBA solutions. Four 4 duplicates of each cement sample types were made
 282 to obtain the given uncertainty values.

283

284 3.3. Results of the PGAA measurements

285 3.3.1. PGAA characterization of the pure OPC and SAC powders.

286 PGAA was used to characterize the elemental compositions of the pure OPC and SAC powders.

287 The results are shown in Table 3.

288

PGAA measurement	Pure OPC	Pure SAC
Element	wt%	wt%
Si	9.62	2.84
Al ₂	2.76	13.3
Fe ₂	2.46	0.72
Mn	0.29	0.10
S	1.29	9.02
Ca	45.2	27.9
Na	0.48	0.53
Ti	0.17	0.23
H	0.11	0.05
B	0.004	0.02
Cl	0.02311	0.11579

289

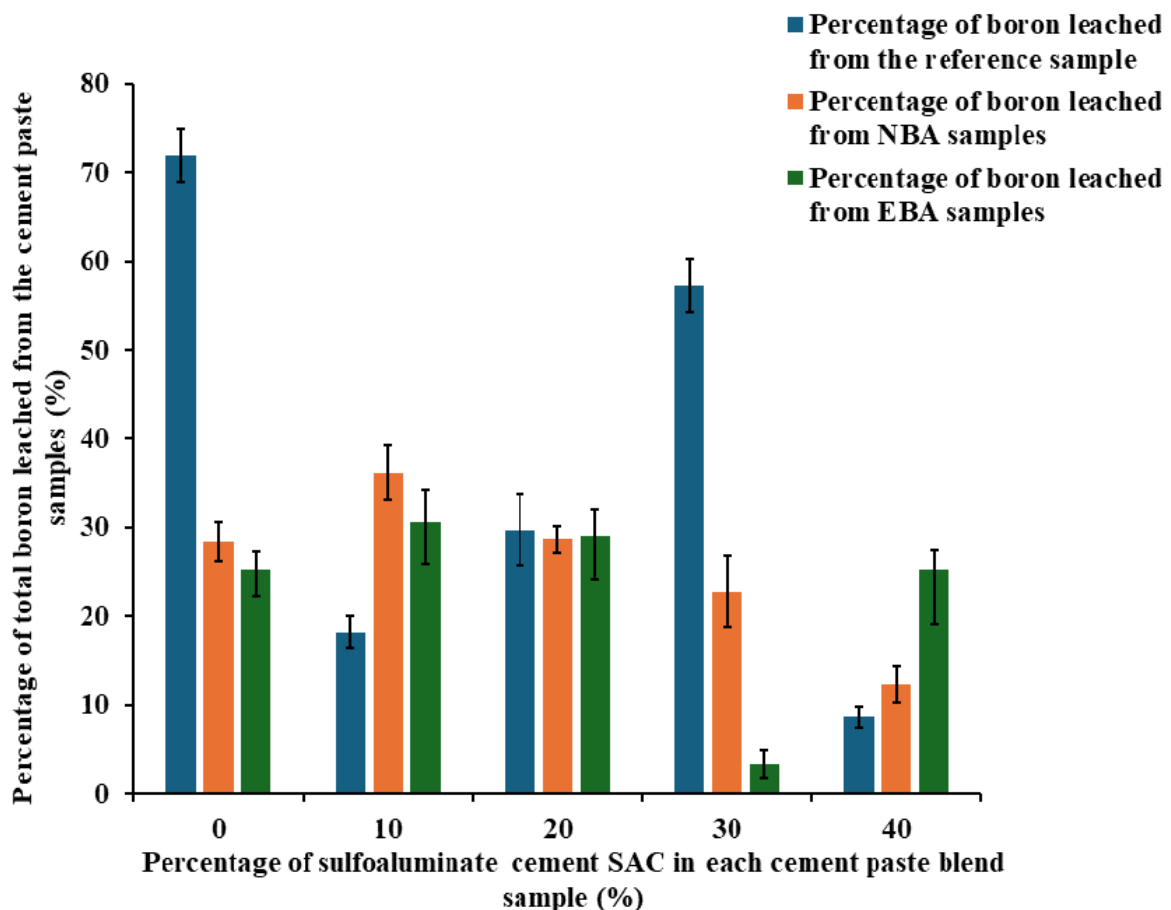
290 **Table 3** PGAA characterization of the elemental compositions of the pure OPC and pure SAC
 291 powders.

292

293 3.3.2. Results of the PGAA measurements of the cement paste samples.

294 The PGAA measured the total boron concentration results of the natural NBA and enriched
 295 EBA borate immobilized cement paste samples which were recalculated from the measured
 296 ^{10}B concentration values in the samples based on the natural boron isotopic ratio (i.e. 80%
 297 ^{11}B :20% ^{10}B). Since it was not possible to directly measure the concentration of ^{11}B using the
 298 PGAA system (due to its very low neutron capture cross section), this method could not be
 299 used to account for the leaching effect on the boron isotopic ratio. Therefore, in this study the
 300 percentage of total boron concentration leached from each cement paste blend sample was
 301 plotted against increasing SAC percentage to assess each samples' characteristic boron
 302 leachability as shown in Fig. 6.

**PGAA: Percentage of total boron leached from cement blend
 paste samples**



303

304

305 **Fig. 6** PGAA: total percentage of boron leached from the cement paste samples against
 306 increasing SAC percentage in the cement paste blend samples.

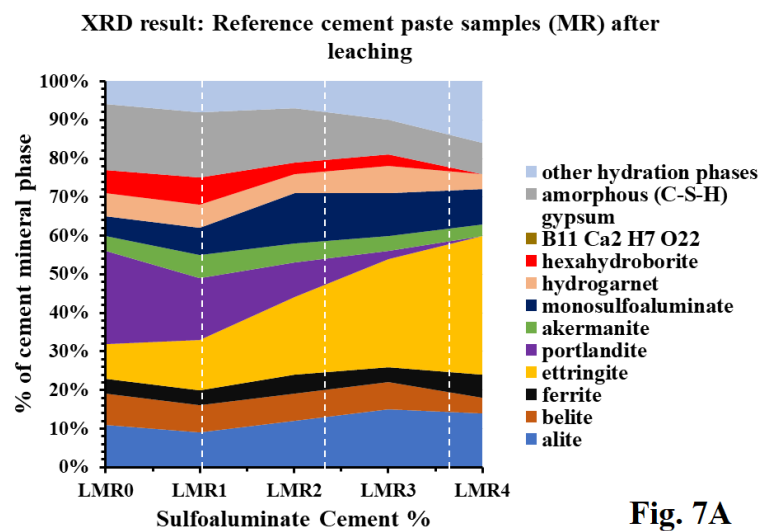
307

308

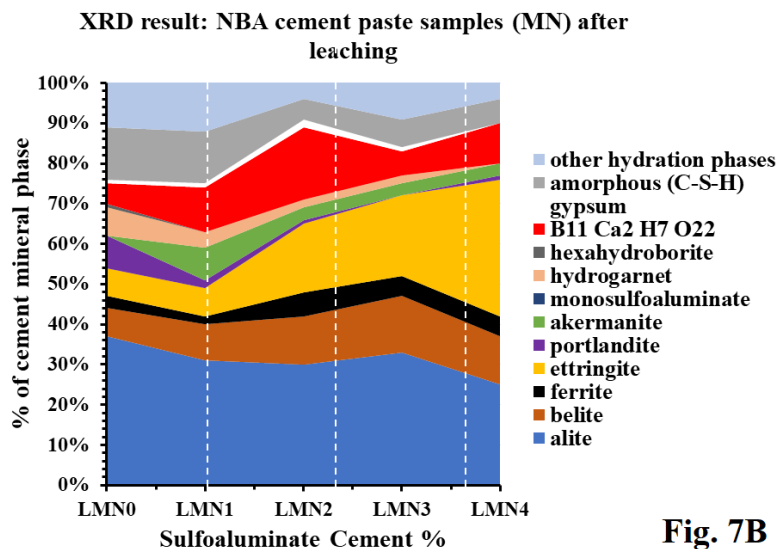
309 **3.4. Results of the XRD measurements**

310 The simulated waste forms' semiquantitative XRD measurements showed percentage changes
 311 in the cement mineral phases as the quantity of SAC increased. The XRD measurements
 312 detected primary cement clinker mineral phases (i.e., alite (Ca_3SiO_5), belite (Ca_2SiO_4) and
 313 calcium aluminoferrite ($\text{Ca}_2(\text{Al}, \text{Fe})_2\text{O}_5$)) and secondary cement hydration mineral phases (i.e.,
 314 ettringite ($\text{Ca}_6\text{Al}_2(\text{SO}_4)_3(\text{OH})_{12} \cdot 2.6\text{H}_2\text{O}$), portlandite ($\text{Ca}(\text{OH})_2$), åkermanite ($\text{Ca}_2\text{Mg}(\text{Si}_2\text{O}_7)$),
 315 monosulfoaluminate ($\text{Ca}_4\text{Al}_2(\text{SO}_4)(\text{OH})_{12} \cdot 6\text{H}_2\text{O}$), hydrogarnet ($\text{Ca}_7(\text{SiO}_4)_3(\text{OH})_2$), gypsum
 316 ($\text{CaSO}_4 \cdot 2\text{H}_2\text{O}$), amorphous (calcium-silicate-hydrate(C-S-H)), and the boron-based hydration
 317 mineral phases hexahydroborite ($\text{CaO} \cdot \text{B}_2\text{O}_3 \cdot 6\text{H}_2\text{O}$) and $\text{B}_{11}\text{Ca}_2\text{H}_7\text{O}_{22}$. Other cement hydration
 318 mineral phases detected in trace amount include mayenite ($\text{Ca}_{12}\text{Al}_{14}\text{O}_{32}[\square_4\text{Cl}_2]$), merwinite
 319 ($\text{Ca}_3\text{Mg}(\text{SiO}_4)_2$), thérnardite (Na_2SO_4), ye'elimite ($\text{Ca}_4\text{Al}_6\text{O}_{12}\text{SO}_4$), and the boron-based
 320 hydration mineral phases inyoite ($\text{CaB}_3\text{O}_3(\text{OH})_5 \cdot 4\text{H}_2\text{O}$) and ulexite ($\text{NaCaB}_5\text{O}_6(\text{OH})_6 \cdot 5\text{H}_2\text{O}$).

321



322



323

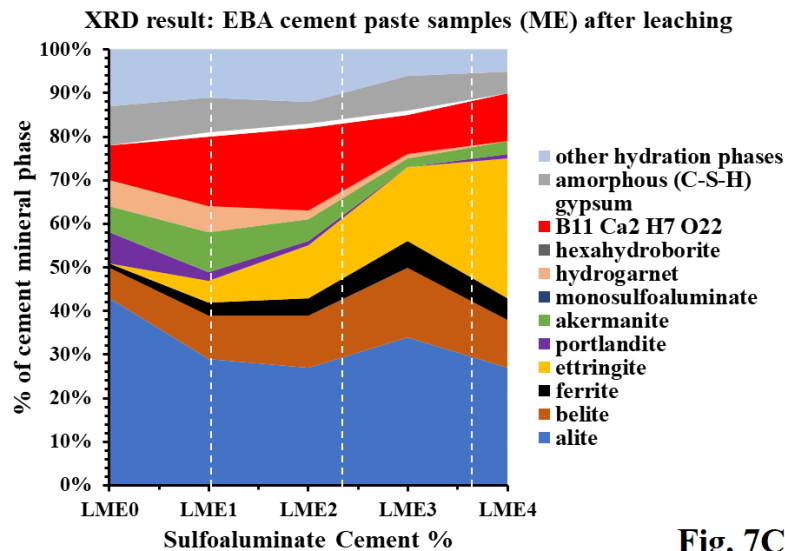


Fig. 7C

324
325
326
327
328
329
330
331

Fig. 7 Percentile (%) changes of cement mineral phases with changing SAC% in the waste forms after the standardized leaching test by XRD measurement in SAC-blend in the reference (MR) i.e. OPC cement mixed with DM water (Fig. 7A), NBA (Fig. 7B) and EBA (Fig. 7C) solutions. (see Table S1b)

332 The XRD results indicate a higher amount of the original clinker phases (alite and belite) present
333 in the NBA and EBA cement-paste samples compared to the reference cement-paste samples.
334 The quantity of the new boron hydration phase $B_{11}Ca_2H_7O_{22}$ is maximum in the 20% SAC/NBA
335 samples (LMN2) 20% SAC/EBA samples (LME2) (see Table S1b) which indicates a
336 connection between the presence of portlandite and ettringite with SAC content.
337

338 3.5. Results of the ICP-OES measurements of the leachates

339 The amount of boron leached from NBA and EBA waste forms was measured by the ICP-OES
340 and presented in Figs. 9A and 9B. The measured values are in the same order of magnitude.
341 The lowest amount of leached boron belonged to the waste forms containing 20% SAC blend
342 for both enriched and natural boric acid containing samples. The average uncertainty value for
343 the ICP-OES measurement was 8%.

344
345
346

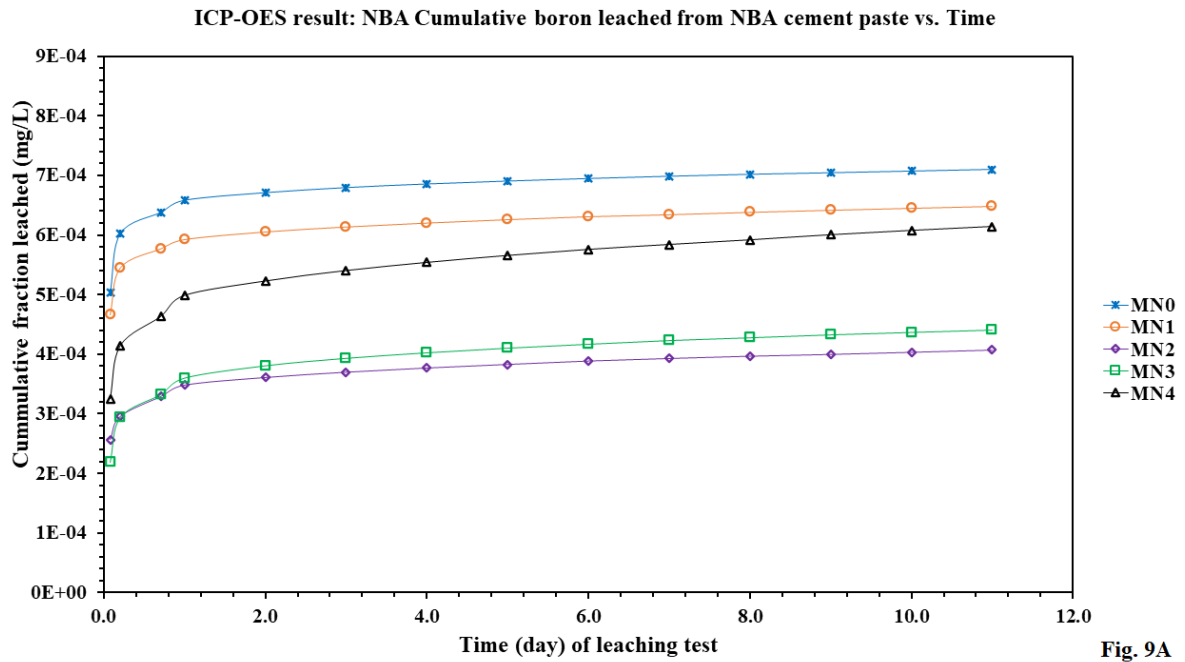


Fig. 9A

347
348
349

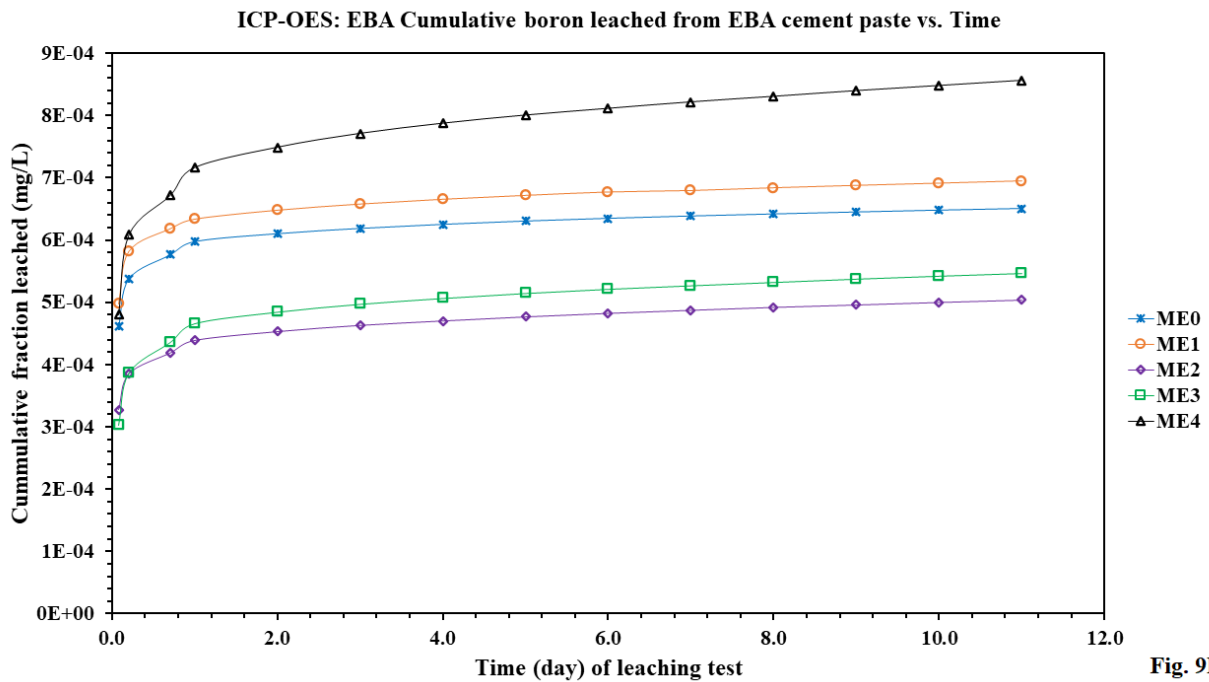


Fig. 9B

350
351
352
353
354
355
356
357
358
359

Fig. 9 ICP-OES analysis of boron leached from the NBA mixed cement paste samples (A) and the EBA mixed cement paste samples (B) during the 11 days standardized leaching test. The ICP-OES results for boron were measured at 8% average uncertainty. ME = EBA cement-paste samples; MN = NBA cement-paste samples; 0 = 0% SAC; 1 = 10% SAC; 2 = 20% SAC; 3 = 30% SAC and 4 = 40% SAC.

360 **3.6. Results of the ICP-MS measurements of the leachates**

361 The isotopic measurement of ^{10}B and ^{11}B [10] leached from the NBA and EBA waste forms
 362 respectively, were analyzed by the ICP-MS. ^{11}B isotope abundance trend (%) results of
 363 measured leachates of the NBA specimens seem to indicate no significant change with increase
 364 in the standardized leaching test time. However, results of the ^{10}B isotope abundance (%)
 365 measurements of the EBA leachate samples indicate a significant reduction of ^{10}B isotope in
 366 the leachate samples with standardized leaching test sampling time. The average relative
 367 uncertainty percent value for the measurement was set at a value of 5% for the boron isotope
 368 measurement.

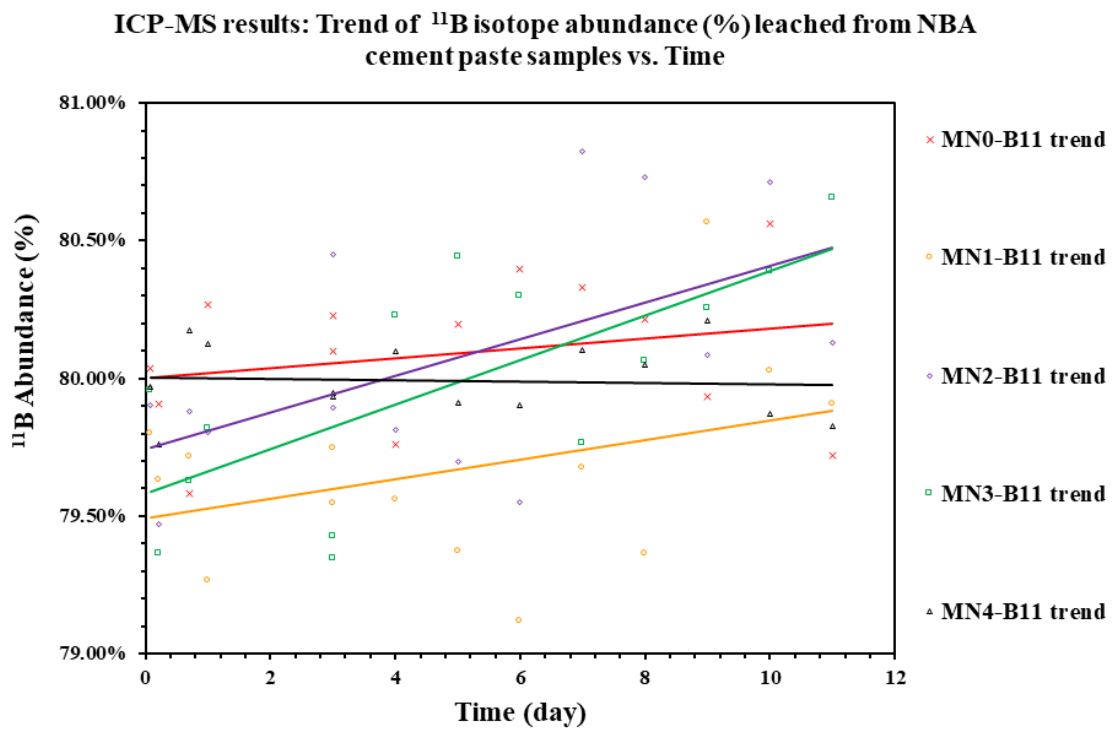
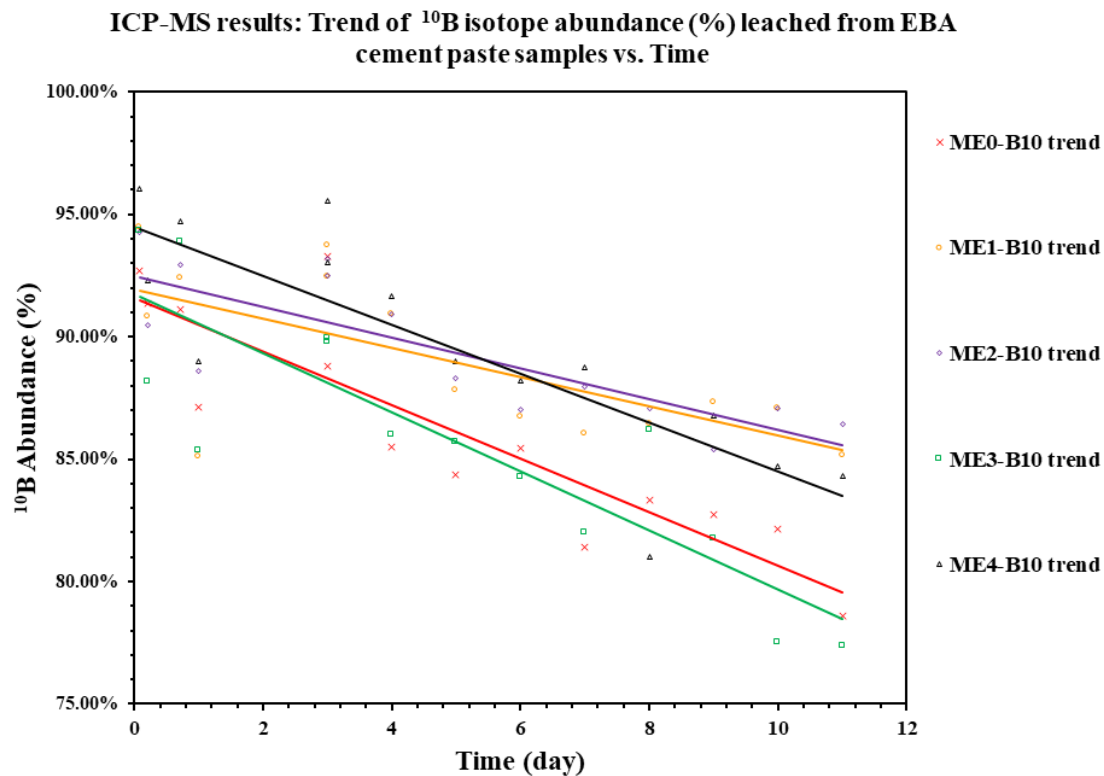


Fig. 10A

369
 370

**Fig. 10B**

371

372

373 **Fig. 10** ICP-MS analysis of boron-11 leached from the NBA mixed cement paste samples (A)
 374 and boron-10 leached from the EBA mixed cement paste samples (B) during the 11 days
 375 standardized leaching test.

376

377

4. Discussions

378

4.1. Physical characteristics of solidified cement paste samples

379

4.1.1. Effect of boron and SAC percentage on surface morphology

380

381 A microstructural study of a previous cementitious matrices research [21] using SEM indicated
 382 that unreacted clinker mineral phases such as alite, belite, and calcium aluminoferrite, appear
 383 brighter while hydrated cement phases appear darker in SEM-BSE images. Our result showed
 384 that when compared to the SAC/NBA and SAC/EBA cement paste samples, the SAC/Reference
 385 cement paste samples showed the least surface fracture value and the least value of surface
 386 unhydrated clinker mineral phases on the cement paste samples (see Figs. 1, 2, 3 and 4).
 387 Furthermore, the SEM surface morphological analyses of the solidified samples before and after
 388 the leaching test (Figs. 1 and 2) appear to suggest that clinker mineral phases were observed
 389 more in the SAC/NBA cement paste samples than in the EBA cement paste samples; implying
 390 a greater borate liquid waste cement hydration retardation in the SAC/NBA cement paste
 samples. This morphological observation might be further reinforced by mineralogical analyses

391 of the XRD results (Figs. 7A, 7B and 7C) which clearly indicated that cement paste samples
392 mixed with the simulated borate waste solutions retained significantly more unhydrated clinker
393 phases than the reference cement-paste samples, with noticeable percentile increase of the
394 unhydrated clinker phases above the 20% SAC point. These morphological results might
395 indicate that the SAC/NBA samples could have a higher boron leachability value than the
396 SAC/Reference and SAC/EBA samples as the greater value of increased unhydrated clinker
397 mineral phases might be an indicator of decreased boron immobilization in the SAC/NBA
398 cement paste matrices due to the NBA's ^{11}B fractionation characteristics of tendency towards
399 the liquid phase which is based on its trigonal planar molecular structure [10]. Furthermore,
400 surface macro-fracture length analyses of the middle section of the solidified cement paste
401 samples (Figs. 3 and 4) indicate that the SAC/NBA and SAC/EBA samples have significantly
402 higher total surface macro-fracture length values than the SAC/Reference–DM Water samples.
403 The increased surface macro-fractures on the boric acid samples could also imply reduced
404 physical stability of the cement matrices and by morphological implication increased boron
405 leachability through these surface fissures.

406 **4.1.2. Effect of boron and SAC percentage on compressive strength**

407 The compressive strength results of this study (Fig. 5) indicated that the reference specimens
408 had higher compressive strength values than both the NBA and EBA ones. This also suggests
409 that the boric acid was impeding the cement hydration process. The samples compressive
410 strength significantly decreased after reaching a 20% SAC peak value. This significant decrease
411 in compressive strength might be attributed to an oversupply of alumina and sulphate from the
412 increasing SAC percentage which would lead to increased production of structurally deleterious
413 cement hydration phases such as gypsum [13]. The 20% SAC/EBA cement paste sample
414 showed the highest compressive strength value among the boric acid cement paste samples;
415 indicating that blending 20% SAC in OPC is the best ratio for cementitious boron
416 immobilization. The NBA cement paste samples show lower compressive strength values than
417 EBA cement samples which might imply that the NBA cement paste samples would show
418 higher boron leachability values. It is important to note that in comparison with the reference
419 samples, the compressive strength measurements of both the NBA and EBA cement paste
420 samples at all SAC addition percentages fall below the BS EN 196-1:2005 standard OPC paste
421 compressive strength at 28 days value of 53 MPa [22].

422

423 **4.2. Effects of boron enrichment and SAC percentage change on the** 424 **mineralogy of the solid cement paste samples**

425 The primary cement mineral (clinker) phases (i.e. alite, belite, and ferrite) accounted for
426 approximately 23% of the total mineral phases in the reference samples, but they are present
427 approx. 45 and 50 % in the NBA and EBA samples, respectively, according to a comparison of
428 the XRD results of the reference samples and the boric acid solidified samples (i.e., NBA
429 samples and EBA samples, as shown in Figs. 7A, 7B, and 7C, respectively). The results also
430 showed that ettringite and C-S-H content is reduced in the NBA and EBA solidified samples
431 compared with reference samples. Furthermore, the result also showed that the new boron-
432 based cement hydration mineral phase $B_{11}Ca_2H_7O_{22}$ (see Fig. 7) makes up a significant
433 percentage in the NBA and EBA cement paste samples. However, it is absent in the reference
434 cement sample where hexahydroborite is detected. It is also observed that the $B_{11}Ca_2H_7O_{22}$
435 showed the highest quantity in the 20% SAC blend making up the total cement mineral phase
436 composition of approximately 16% in the EBA cement paste sample (LME2) and
437 approximately 14% in the NBA cement paste sample (LMN2); this implies that ^{10}B (EBA)
438 samples shows greater immobilization value than the ^{11}B (NBA) samples.

439 Though reduced in the EBA and NBA cement samples when compared to the reference sample,
440 the cement hydration mineral phases ettringite and C-S-H - which was shown to potentially act
441 as a host to boron ions and major cement binding phases [23] (both crucial for cementitious
442 immobilization) were formed in both the NBA and EBA cement samples. The formation of
443 ettringite appeared to increase with the supply of alumina (ye'elimite and tetracalcium
444 aluminoferrite) from the percentage increase of SAC in the cement paste samples. The boron
445 cement hydration mineral phase $B_{11}Ca_2H_7O_{22}$ might be inferred to be the major form of boron
446 immobilization in the cement paste samples mixed with boric acid. It was observed that
447 $B_{11}Ca_2H_7O_{22}$ formation peaked at 20% SAC blend in both the NBA and EBA samples. This
448 could imply that 20% SAC blend in OPC might be the optimal blend ratio for cementitious
449 boron immobilization.

450 **4.3. Borate immobilization (boron uptake) mechanism effect on ettringite** 451 **and C-S-H formation**

452 When ettringite ($Ca_6Al_2(SO_4)_3(OH)_{12}.26H_2O$) is synthesized in the presence of high
453 concentrations of borate, borate uptake takes place via chemical adsorption at the surface
454 interface of the precipitated gelatinous ettringite which is produced as the borate ions i.e.

455 B(OH)_4^- are substituted by the SO_4^{2-} ions in the ettringite. When the ratio of the concentration
456 of borate ions to SO_4^{2-} ions in the cement paste system is greater than 1, there is decomposition
457 of the ettringite with a consequent production of the amorphous C-S-H gel which acts as the
458 binder phase [24].

459 **4.4. Effects of SAC percentage and boron enrichment on boron leachability**

460 The PGAA analyses showed the percentage of total boron concentration leached from the
461 cement paste samples with changing percentage of SAC and indicated that the reference, NBA
462 and EBA cement paste samples all showed different boron leachability characteristics. The
463 PGAA characterization elemental measurement showed that the pure SAC had four times more
464 boron content than the pure OPC. The reference samples showed the highest percentage change
465 in relative boron leached as the pure OPC reference sample leached over 70% of boron from its
466 matrices while the other pure OPC samples immobilizing the borate solutions leached below
467 30% of boron in their matrices. However, as SAC was initially added to the reference sample,
468 there was a 50% drop of boron leaching. Furthermore, as the reference was supplied with
469 increasing percentage of SAC an increase in boron leached was observed. Both the NBA and
470 EBA cement paste samples indicated lower relative boron leachability rates values with
471 increasing SAC than the reference samples. About 30% percent of boron was leached from all
472 the cement samples at the 20% SAC blend.

473 The ICP-OES analyses of cumulative fraction of boron leached CFL with time (11 days) from
474 the solidified samples (Fig. 9) of the NBA and EBA sample leachates showed that the measured
475 values were in the same order of magnitude, but the values were different, the magnitude of the
476 difference was shown to be consistent with the SAC content percentage in the cement paste
477 samples. If the cementitious system did not contain SAC, typically 10% higher CFL boron was
478 measured in both the NBA and EBA samples. As the fraction of SAC increased, the trend
479 reversed, and the amount of leached boron also increased. This suggest that the lowest amount
480 of leached boron-ion belong to the cement-paste mixtures containing 20% SAC for both
481 enriched and natural boric acid containing samples. The low boron leaching at 20% SAC might
482 imply that boron immobilizing hydration phases i.e. ettringite are quantitatively formed at this
483 blend ratio. The substitution of SO_4^{2-} with B(OH)_4^- , which occurs at the surface layer of
484 ettringite, is inferred to be the cause of the decreased boron uptake in ettringite when it is
485 synthesized in the presence of H_3BO_3 solution [24]. Furthermore, increased supply of

486 $[\text{Al}(\text{OH})_4]^-$ from the SAC leads to an increase in amorphous phase (CSH) production as other
487 cement hydration matrix phases formed by ettringite-based waste forms, such as gypsum and
488 portlandite, function as buffers against $(\text{OH})^-$ (i.e. pH) of the borate, calcium, aluminate, and
489 sulphate species' in the contacting solution [25].

490 The ICP-MS analyses used to study the trends of $^{11}\text{B}/^{10}\text{B}$ ratio leached from NBA and EBA
491 samples indicated a reduction in the trend of ^{10}B abundance leached from the EBA cement
492 samples into the leachates with time. However, the trend of ^{11}B abundance leached from the
493 NBA cement samples did not show any marked change with time over the sampling period (see
494 Fig. 10). These results might reinforce the previous research [10] that hypothesized that boron
495 leachability from cementitious matrices used for the immobilization of boric acid liquid waste
496 is related to the molecular structure and isotopic preferences as ^{10}B isotopes have preference
497 for the tetrahedral $\text{B}(\text{OH})_4^-$ molecular structure whereas ^{11}B isotopes have a preference for the
498 trigonal planar $\text{B}_5\text{O}_6(\text{OH})_4^-$ [10]. This could influence boron immobilization as the ^{10}B hosting
499 tetrahedral molecular structure is retained within the structure of the cementitious matrices
500 phase as their structure is analogous to SiO_4^{4-} within the matrices, while the ^{11}B hosting trigonal
501 molecular structure are more mobile and can be leached easier into the liquid phase.

502

503 **5. Conclusions**

504 Borate cement samples (NBA and EBA) showed more presence of unhydrated mineral phases
505 and surface macro-fracture than the reference cement samples as the borate solutions were
506 shown to retard the cement hydration process.

507 Both NBA and EBA solidified samples showed lower compressive strength values than the
508 reference cement samples. However, among the boric acid solidified samples, the 20% SAC
509 blend/EBA samples indicate the highest compressive strength values as it showed the optimal
510 physical and chemical stability compared with all the other OPC/SAC blends.

511 PGAA results showed that the borate immobilized samples NBA and EBA showed lesser
512 relative boron leachability rates than the reference samples. XRD study of the solidified
513 wastefoms showed that the simulated borate waste solutions (NBA and EBA) retarded the
514 cement hydration process with the formation of a new boron-based cement hydration mineral
515 phase $\text{B}_{11}\text{Ca}_2\text{H}_7\text{O}_{22}$ observed to be a significant mechanism for boron immobilization alongside

516 ettringite in the cementitious matrices with the 20% SAC blend/EBA sample showing the
517 highest production of this phase.

518 ICP-OES analyses of boron leached from the cement paste samples into the leachates during
519 the standardized leaching test indicated that the boric acid cement samples (NBA and EBA)
520 mixed with 20% SAC blend seemed to show the least values of boron leached. While isotopic
521 analyses of the ICP-MS results of leachates from the standardized leaching test seemed to
522 indicate ^{10}B abundance trend seemed to reduce in the leachates from the EBA cement samples
523 with time but there was no significant change of ^{11}B abundance trend in the leachates from the
524 NBA cement samples.

525 The conclusive inference from the study indicate that 20% SAC blended into 80% OPC is
526 optimal cement ratio for boron immobilization.

527

528 **Acknowledgements**

529 This research was supported by HUN-REN Centre for Energy Research Budapest, Hungary
530 (Dedicated to the memory of our colleague and friend Mihaly Óvári); CEMKUT Research and
531 Development Ltd. Budapest, Hungary; the Tempus Stipendium Hungaricum Program (SHE-
532 46160-004/2021) and the Doctoral School of Environmental Sciences Eötvös Loránd
533 University Budapest, Hungary. MF is grateful to the János Bolyai Research Scholarship
534 provided by the Hungarian Academy of Sciences. GI is gratitude to all members of Lithosphere
535 Fluid Research Group (LRG).

536

537

538 **References**

- 539 [1] F. Chien, L. Huang, and W. Zhao, “The influence of sustainable energy demands on
540 energy efficiency: Evidence from China,” *J. Innov. Knowl.*, vol. 8, no. 1, p. 100298,
541 Jan. 2023, doi: 10.1016/J.JIK.2022.100298.
- 542 [2] S. Dorahaki, M. Rashidinejad, A. Abdollahi, and M. Mollahassani-pour, “A novel two-
543 stage structure for coordination of energy efficiency and demand response in the smart
544 grid environment,” *Int. J. Electr. Power Energy Syst.*, vol. 97, pp. 353–362, Apr. 2018,
545 doi: 10.1016/J.IJEPES.2017.11.026.
- 546 [3] M. Sadiq, T. Q. Ngo, A. A. Pantamee, K. Khudoykulov, T. Thi Ngan, and L. P. Tan,
547 “The role of environmental social and governance in achieving sustainable

- 548 development goals: evidence from ASEAN countries,”
549 [http://www.tandfonline.com/action/authorSubmission?journalCode=rero20&page=ins](http://www.tandfonline.com/action/authorSubmission?journalCode=rero20&page=instructions)
550 [tructions](http://www.tandfonline.com/action/authorSubmission?journalCode=rero20&page=instructions), vol. 36, no. 1, pp. 170–190, 2022, doi: 10.1080/1331677X.2022.2072357.
- 551 [4] W. Chen, X. Ling, Q. Li, B. Yuan, B. Li, and H. Ma, “Experimental evidence on
552 formation of ulexite in sulfoaluminate cement paste mixed with high concentration
553 borate solution and its retarding effects,” *Constr. Build. Mater.*, vol. 215, pp. 777–785,
554 2019, doi: 10.1016/j.conbuildmat.2019.04.242.
- 555 [5] J. Xu and W. Zhang, “The application of 10B enriched boric acid in nuclear power
556 industry,” *Int. Conf. Nucl. Eng. Proceedings, ICONE*, vol. 3, pp. 1–5, 2010, doi:
557 10.1115/icone18-29042.
- 558 [6] A. Palomo and J. I. López de la Fuente, “Alkali-activated cementitious materials:
559 Alternative matrices for the immobilisation of hazardous wastes - Part I. Stabilisation
560 of boron,” *Cem. Concr. Res.*, vol. 33, no. 2, pp. 281–288, 2003, doi: 10.1016/S0008-
561 8846(02)00963-8.
- 562 [7] Q. Sun and J. Wang, “Cementation of radioactive borate liquid waste produced in
563 pressurized water reactors,” *Nucl. Eng. Des.*, vol. 240, no. 10, pp. 3660–3664, 2010,
564 doi: 10.1016/j.nucengdes.2010.07.018.
- 565 [8] O. Gorbunova, “Cementation of liquid radioactive waste with high content of borate
566 salts,” *J. Radioanal. Nucl. Chem.*, vol. 304, no. 1, pp. 361–370, 2015, doi:
567 10.1007/s10967-014-3886-3.
- 568 [9] N. R. Rakhimova, R. Z. Rakhimov, V. P. Morozov, L. I. Potapova, and Y. N. Osin,
569 “Mechanism of solidification of simulated borate liquid wastes with sodium silicate
570 activated slag cements,” *J. Clean. Prod.*, vol. 149, pp. 60–69, 2017, doi:
571 10.1016/j.jclepro.2017.02.066.
- 572 [10] M. Rostamiparsa *et al.*, “The geochemical role of B-10 enriched boric acid in cemented
573 liquid radioactive wastes,” *J. Radioanal. Nucl. Chem.*, vol. 332, no. 7, pp. 2543–2557,
574 2023, doi: 10.1007/s10967-023-08913-5.
- 575 [11] Q. Sun, J. Li, and J. Wang, “Effect of borate concentration on solidification of
576 radioactive wastes by different cements,” *Nucl. Eng. Des.*, vol. 241, no. 10, pp. 4341–
577 4345, Oct. 2011, doi: 10.1016/J.NUCENGDES.2011.08.040.
- 578 [12] Q. Sun and J. Wang, “Cementation of radioactive borate liquid waste produced in
579 pressurized water reactors,” *Nucl. Eng. Des.*, vol. 240, no. 10, pp. 3660–3664, Oct.
580 2010, doi: 10.1016/J.NUCENGDES.2010.07.018.
- 581 [13] K. Pimraksa and P. Chindapasirt, “Sulfoaluminate cement-based concrete,” *Eco-
582 efficient Repair Rehabil. Concr. Infrastructures*, pp. 355–385, Jan. 2018, doi:
583 10.1016/B978-0-08-102181-1.00014-9.
- 584 [14] Y. Xie and C. Qian, “Improved ettringite stabilization by calcium carbonate and
585 calcium nitrate additions in ternary PC-CSA-C\$ systems,” *Cem. Concr. Res.*, vol. 175,
586 p. 107383, Jan. 2024, doi: 10.1016/J.CEMCONRES.2023.107383.
- 587 [15] ASTM international, “C1308-08, Standard Test Method for Accelerated Leach Test for
588 Diffusive Releases from Solidified Waste.” 2017.

- 589 [16] M. Rostamiparsaa, “The geochemical role of B-10 enriched boric acid in cemented
590 liquid radioactive wastes,” *J. Radioanal. Nucl. Chem.*, 2023.
- 591 [17] B. Gaël, T. Christelle, E. Gilles, G. Sandrine, and S. F. Tristan, “Determination of the
592 proportion of anhydrous cement using SEM image analysis,” *Constr. Build. Mater.*,
593 vol. 126, pp. 157–164, 2016, doi: 10.1016/j.conbuildmat.2016.09.037.
- 594 [18] G. L. Molnar, *Handbook of Prompt Gamma Activation Analysis with Neutron Beams*,
595 vol. 269, no. 43. 1994.
- 596 [19] Z. Révay, “Determining elemental composition using prompt γ activation analysis,”
597 *Anal. Chem.*, vol. 81, no. 16, pp. 6851–6859, Aug. 2009, doi:
598 10.1021/AC9011705/ASSET/IMAGES/AC-2009-011705_M024.GIF.
- 599 [20] EN196-1, “Methods of testing cement - Part 1: Determination of strength,” *Eur. Stand.*,
600 pp. 1–33, 2005.
- 601 [21] H. F. W. Taylor, *Cement Chemistry*. 1990. doi: 10.1142/9781860949982_0010.
- 602 [22] B. Standard, “British Standard Methods of testing cement —,” vol. 3, no. August,
603 2003.
- 604 [23] M. L. D. Gougar, B. E. Scheetz, and D. M. Roy, “Ettringite and C_3S/H Portland
605 cement phases for waste ion immobilization: A review,” *Waste Manag.*, vol. 16, no. 4,
606 pp. 295–303, Jan. 1996, doi: 10.1016/S0956-053X(96)00072-4.
- 607 [24] Y. Hiraga and N. Shigemoto, “Boron uptake behavior during ettringite synthesis in the
608 presence of H_3BO_3 and in a suspension of ettringite in H_3BO_3 ,” *J. Chem. Eng. Japan*,
609 vol. 43, no. 10, pp. 865–871, 2010, doi: 10.1252/jcej.10we160.
- 610 [25] G. J. McCarthy, D. J. Hassett, and J. A. Bender, “Synthesis, Crystal Chemistry and
611 Stability of Ettringite, A Material with Potential Applications in Hazardous Waste
612 Immobilization,” *MRS Proc.*, vol. 245, pp. 129–140, 1991, doi: 10.1557/proc-245-129.
- 613